BIFURCATIONS OF FINITE DIFFERENCE SCHEMES AND THEIR APPROXIMATE INERTIAL FORMS

ROLF BRONSTERING AND MIN CHEN

ABSTRACT. In this paper, we show that the bifurcation diagrams of finite difference semidiscretizations of certain dissipative parabolic partial differential equations can be well approximated by their approximate inertial forms (AIFs) when a set of second-order, L^2-orthogonal incremental unknowns is used.

1. INTRODUCTION

Inertial-multigrid-algorithm is proposed for the long time approximation of solutions of dissipative systems because it offers flexibility and better stability which results in a better efficiency (cf. [3], [6], [17] and references therein). Suppose that $\mathcal{V}$ is the solution space of the differential equation and $\mathcal{V}_h$ is the approximate solution space under standard finite difference. In the cases that the dimension of $\mathcal{V}_h$ has to be very large to describe the fine structure of the solution, the inertial-multigrid-algorithm can be used to save the CPU time and/or the memory. The scheme is based on decomposing $\mathcal{V}_h$ into $\mathcal{V}_h = \mathcal{P}_h \oplus \mathcal{Q}_h$, where $\mathcal{P}_h$ corresponds to a coarse grid approximation of $\mathcal{V}$ and $\mathcal{Q}_h$ is the complement of $\mathcal{P}_h$ containing only short-wavelength components (cf. [4] and [5]). Hence for any $u_h \in \mathcal{V}_h$, one can decompose u_h into

$$u_h = y_h + z_h\,,$$

where $y_h \in \mathcal{P}_h$ approximates the long-wavelength part of the solution and $z_h \in \mathcal{Q}_h$ approximates the short-wavelength part of the solution. Following the theory of inertial manifolds, the short-wavelength component z_h carries only a small part

AMS subject classifications: 35A40, 65M06.

of the total energy, therefore, some terms involving z_h can be neglected. The motivation of the scheme can be best described as that *in the cases that extremely fine grids are required for the numerical simulation, one can take into account the effect of small scale terms in an efficient way, instead of simply adding more mesh points.* This reasoning leads to the inertial multigrid algorithm: A primary advantage of this algorithm is that it provides $\mathcal{V}_h$-accuracy with $\mathcal{P}_h$-computational complexity, and has better numerical stability properties than a direct discretization using $\mathcal{V}_h$ (cf. [6]). Numerical results obtained by [2] confirmed that the algorithm indeed provides $\mathcal{V}_h$-accuracy when used to simulate the solution of reaction diffusion equations in one-, two-, and three-space dimensions and when used on the one-dimensional Kuramoto-Sivashinsky equation.

In this paper, we study the bifurcation diagram of the scheme and compare it with that of the underlying continuous problem and that of the standard finite difference scheme. In practice, this means examining the numerical method for a large range of physical parameters at once rather than just looking at convergence for a fixed set of parameters. Thus, this analysis aims toward proving convergence to a bifurcation diagram rather than to a single solution. As an example, we will study the inertial multigrid algorithm for the reaction-diffusion equation and Kuramoto-Sivashinsky equation.

A new set of incremental unknowns, which is L^2-orthogonal and second-order, is used in our study. For a one-dimensional problem on $\Omega = [a, b]$ with zero Dirichlet boundary condition we set $h = (b - a)/(N + 1)$ where $N = 2n + 1$. Suppose u_i approximates the solution $u(x)$ at mesh points x_i, where $x_i = a + ih$ and $1 \leq i \leq N$, so the unknowns are $u_h = (u_1, \cdots, u_N)^T \in \mathbb{R}^N$. The new set of incremental

unknowns is defined by

$$\begin{aligned} p_i &= \frac{1}{4}(u_{2i-1} + 2u_{2i} + u_{2i+1}), \quad i = 1, \ldots, n, \\ q_i &= \frac{1}{4}(-u_{2i-2} + 2u_{2i-1} - u_{2i}), \quad i = 1, \ldots, n+1, \end{aligned} \tag{1.1}$$

where p_i is an average value of $u(x)$ in the neighborhood of $x = x_{2i}$ and q_i is an increment of $u(x)$ in the neighborhood of $x = x_{2i-1}$. If one expands q_i at x_{2i-1} by Taylor's formula and assumes the solution $u(x)$ is smooth, it is easy to see that $q_i = O(h^2)$ and in which sense that we say this set of incremental unknowns is second-order.

Let $\mathcal{P}_h$ and $\mathcal{Q}_h$ be subspaces of $\mathbb{R}^N$ where

$$\begin{aligned} \mathcal{P}_h &= \left\{ u_h \in \mathbb{R}^{2n+1} \middle| \quad -u_{2i-2} + 2u_{2i-1} - u_{2i} = 0, \quad i = 1, \ldots, n+1 \right\}, \\ \mathcal{Q}_h &= \left\{ u_h \in \mathbb{R}^{2n+1} \middle| \quad u_{2i-1} + 2u_{2i} + u_{2i+1} = 0, \quad i = 1, \ldots, n \right\}. \end{aligned} \tag{1.2}$$

Since $\mathcal{P}_h$ is defined by $n+1$ linearly independent constraints, $\dim \mathcal{P}_h = N-(n+1) = n$. Likewise, $\dim \mathcal{Q}_h = n+1$. One can also show that $\mathcal{P}_h$ and $\mathcal{Q}_h$ are orthogonal to each other since for any $y_h \in \mathcal{P}_h$ and $z_h \in \mathcal{Q}_h$

$$\begin{aligned} 2\langle y_h, z_h \rangle &= 2\sum_{i=1}^{2n+1} y_i z_i = 2\sum_{i=1}^{n+1} y_{2i-1} z_{2i-1} + 2\sum_{i=1}^{n} y_{2i} z_{2i} \\ &= \sum_{i=1}^{n+1} (y_{2i-2} + y_{2i}) z_{2i-1} - \sum_{i=1}^{n} y_{2i}(z_{2i-1} + z_{2i+1}) \\ &= \left(\sum_{i=1}^{n+1} y_{2i-2} z_{2i-1} - \sum_{i=1}^{n} y_{2i} z_{2i+1} \right) + \left(\sum_{i=1}^{n+1} y_{2i} z_{2i-1} - \sum_{i=1}^{n} y_{2i} z_{2i-1} \right) \\ &= y_0 z_1 + y_{2n+2} z_{2n+1} = 0 \end{aligned}$$

according to the zero boundary conditions. Hence $\mathbb{R}^N = \mathcal{P}_h \oplus \mathcal{Q}_h$ is a L_2-orthogonal decomposition.

In section 2, we will show that for any $u_h = (u_1, \ldots, u_{2n+1})^T \in \mathbb{R}^N$, there is an unique decomposition

$$u_h = y_h + z_h$$

where $y_h \in \mathcal{P}_h$ depends only on $p = (p_1, \ldots, p_n)^T$ and $z_h \in \mathcal{Q}_h$ depends only on $q = (q_1, \ldots, q_{n+1})^T$. We therefore say that the incremental unknowns defined in (1.1) is L^2-orthogonal.

Comparing with the existing incremental unknowns, one finds that the wavelet-like incremental unknowns is L^2-orthogonal, but of first-order only; and the second-order incremental unknown is second-order, but not L^2-orthogonal (cf. [5]). The advantages of this set of incremental unknowns comes with a price which is that the inverse transform of (1.1) is not local anymore, which means that for any given p and q, one has to solve a system of linear equations to find the corresponding u_h.

The paper is organized is the following way. In section two, we will introduce general space decompositions based on finite difference semidiscretizations and derive the AIF based on that decomposition. In section 3 we prove that the primary bifurcation values of the AIF are the same as those of the original finite difference scheme. Finally, in section 4, we will present the bifurcation diagrams of the discretized reaction-diffusion equation and Kuramoto-Sivashinsky equation.

2. General space decompositions

We consider evolution equations of the form

$$u_t + Au + F(u) = 0, \quad u(0) = u_0 \in \mathcal{V} \tag{2.1}$$

where $\mathcal{V}$ is a Hilbert space (possibly infinite–dimensional), $u(t)$ is the unknown function, A is a symmetric (possibly unbounded) linear operator on $\mathcal{V}$, and F is a nonlinear operator on $\mathcal{V}$.

Assuming that there exists a convergent finite difference semidiscretization for this problem, one can approximate (2.1) by a system of ordinary differential equations

$$(u_h)_t + A_h u_h + F_h(u_h) = 0, \quad u_h(0) = (u_0)_h \in \mathcal{V}_h = \mathbb{R}^N, \tag{2.2}$$

where N is the number of (inner) grid points. The reaction–diffusion equation and the Kuramoto-Sivashinsky equation we will study in section 4 both satisfy the above abstract form. To simplify the notation, the index h will be dropped throughout the rest of this paper, that is, we will use the symbols u, A, F, $\mathcal{P}$, $\mathcal{Q}$ etc. instead of u_h, A_h, F_h, $\mathcal{P}_h$, $\mathcal{Q}_h$. The equation to be considered is thus the ordinary differential equation

$$u_t + Au + F(u) = 0, \quad u(0) = u_0 \in \mathbb{R}^N. \tag{2.3}$$

Introducing the new variable $p \in \mathbb{R}^n$ and $q \in \mathbb{R}^{n+1}$ from the L^2–orthogonal decomposition of $\mathbb{R}^N$ defined in (1.1) and writing them in the matrix form, one has

$$p = V^T u, \quad q = W^T u \tag{2.4}$$

where $u = (u_1, u_2, \cdots, u_N)^T$, $p = (p_1, \cdots, p_n)^T$, $q = (q_1, \cdots, q_{n+1})^T$, $V \in \mathbb{R}^{N\times n}$, $W \in \mathbb{R}^{N\times(n+1)}$ (see page 11 for the explicit shape of V, W). Let T be the operator

$$T = VV^T + WW^T,$$

one finds that

$$Tu = Vp + Wq.$$

Since the matrices V and W have maximal rank, V^TV and W^TW are invertible. Noticing also that the column vectors in V are orthogonal to the column vectors of W, namely, $V^TW = 0$ and $W^TV = 0$, one can prove that T is invertible. The inverse relation of (2.4) (or (1.1)) is therefore

$$u = T^{-1}Vp + T^{-1}Wq \ (\equiv y_h + z_h) \tag{2.5}$$

We now show that formula (2.5) defines a unique decomposition of u with respect to $\mathbb{R}^N = \mathcal{P} \oplus \mathcal{Q}$, that is, we show that for any $p \in \mathbb{R}^n$ and $q \in \mathbb{R}^{n+1}$, $T^{-1}Vp \in \mathcal{P}$ and $T^{-1}Wq \in \mathcal{Q}$. Notice that

$$\mathcal{P} = \left\{ u \mid W^T u = 0 \right\}, \quad \mathcal{Q} = \left\{ u \mid V^T u = 0 \right\}. \tag{2.6}$$

For any $p \in \mathbb{R}^n$, let $v = V(V^TV)^{-1}p$, one can check that $Vp = Tv$ and $W^Tv = 0$ which implies that $v = T^{-1}Vp \in \mathcal{P}$. The proof for $T^{-1}Wq \in \mathcal{Q}$ proceeds analogously.

Remark 2.1. Since $V^TW = 0$ and $W^TV = 0$, the columns of V and W are a basis of $\mathcal{P}$ and $\mathcal{Q}$ respectively. Therefore, for any $u \in \mathbb{R}^N$ one can find unique $\tilde{p} \in \mathbb{R}^n$, $\tilde{q} \in \mathbb{R}^{n+1}$ with $u = V\tilde{p} + W\tilde{q}$.

Substituting (2.5) into (2.3) and applying V^TT (and W^TT) from left we obtain after exploiting the orthogonality of the decomposition

$$\begin{aligned} V^TVp_t + V^TT(Au + F(u)) &= 0, \\ W^TWq_t + W^TT(Au + F(u)) &= 0, \\ p(0) = V^Tu_0\,, \quad q(0) &= W^Tu_0\,, \end{aligned} \tag{2.7}$$

where $u = T^{-1}(Vp + Wq)$. In the cases that A and T are commutable, i.e. $AT = TA$, (2.7) can be written as

$$\begin{aligned} V^TVp_t + V^TAVp + V^TAWq + f(p,q) &= 0, \\ W^TWq_t + W^TAVp + W^TAWq + g(p,q) &= 0, \\ p(0) = V^Tu_0\,, \quad q(0) &= W^Tu_0\,, \end{aligned} \tag{2.8}$$

where $V^TAV \in \mathbb{R}^{n\times n}$, $W^TAW \in \mathbb{R}^{(n+1)\times(n+1)}$, $V^TAW \in \mathbb{R}^{n\times(n+1)}$, $W^TAV \in \mathbb{R}^{(n+1)\times n}$ and

$$f(p,q) := V^TTF(T^{-1}(Vp + Wq)), \quad g(p,q) := W^TTF(T^{-1}(Vp + Wq)). \tag{2.9}$$

Since (2.8) is equivalent to (2.3), the AIF (c.f. [9]) can be defined by neglecting the time derivative q_t in (2.8) and performing one fixed point iteration step for the resulting nonlinear algebraic equation, starting with $q = 0$. If we assume that

W^TAW is invertible, the AIF is

$$p_t + (V^TV)^{-1}(V^TAVp + V^TAW\phi(p) + f(p,\phi(p))) = 0,$$
$$q = \phi(p) = -(W^TAW)^{-1}(W^TAVp + g(p,0)), \tag{2.10}$$
$$p(0) = V^Tu_0.$$

Remark 2.2. When (2.10) is used for the numerical simulation of a solution, the first equation corresponds to the coarse grid approximation and the second equation corresponds to a nonlinear correction of the coarse grid approximation. In order for the algorithm to be numerically efficient, W^TAW has to be well conditioned. Since space $\mathcal{Q}$ is used to approximate the high modes of the eigenspace of A, we can expect W^TAW is well conditioned. In the examples considered in section 4 we can prove that $0 < \mu_1|q|^2 \le \langle AWq, Wq\rangle \le \mu_2|q|^2$ which results $\mathrm{cond}(W^TAW) = \mu_2/\mu_1$ being bounded from above by a constant which does not depend on h.

3. The linear part

Assume now that A and/or F in (2.3) depends on a parameter θ and that $F(0) = D_uF(0) = 0$. Then $u = 0$ is the trivial solution for all θ. To find primary bifurcation values, that is, values of θ at which branches of nontrivial stationary solutions bifurcate from $u = 0$, the first thing to do is to examine the linear part of (2.3) at $u = 0$, that is, A. By the implicit function theorem, only those θ for which A becomes singular can be bifurcation values.

In order for the above reduction to an AIF to be accurate, we expect that the primary bifurcation values of (2.10) are "close" to those of the original system (2.3), or in other words, that the singular values of the linear part $\bar{A}$ of (2.10) are "close" to those of A.

In the cases that $|F(u)| = O(|u|^2)$, $\bar{A}$ can be computed easily. $|F(u)| = O(|u|^2)$ yields $|g(p,0)| = O(|p|^2)$ and $\phi(p) = -(W^TAW)^{-1}W^TAVp +$

(higher order terms in p). It is easy to show that this implies $|f(p,\phi(p))| = O(|p|^2)$. As a consequence, the linear part of (2.10) at $p = 0$ is given by

$$\bar{A} = (V^T V)^{-1}(V^T AV - V^T AW(W^T AW)^{-1}W^T AV). \tag{3.1}$$

We now prove the following result about the singular values of A and $\bar{A}$:

Lemma 3.1. *$\bar{A}$ is singular if and only if A is singular, provided $W^T AW$ is invertible.*

Proof. First, we note that $\bar{A}$ can be written as

$$\bar{A} = (V^T V)^{-1}V^T AP_A V = (V^T V)^{-1}V^T \bar{P}_A AV$$

where

$$P_A = I - Q_A, \quad Q_A = W(W^T AW)^{-1}W^T A,$$
$$\bar{P}_A = I - \bar{Q}_A, \quad \bar{Q}_A = AW(W^T AW)^{-1}W^T.$$

"$\Rightarrow$": Let $\bar{A}$ be singular, then there exists a $p \neq 0$, $\bar{A}p = 0$. It follows that $V^T\bar{P}_A AVp = 0$, so $\bar{P}_A AVp \in \mathcal{Q}$. Using the definition of $\bar{P}_A$, it is easy to see that $W^T\bar{P}_A AVp = 0$. Hence $\bar{P}_A AVp \in \mathcal{P} \cap \mathcal{Q}$ which yields $\bar{P}_A AVp = 0$. If A was not singular, then from $AP_A Vp = \bar{P}_A AVp = 0$, one has $P_A Vp = 0$ so $V^T P_A Vp = V^T Vp = 0$ and $p = 0$ because $V^T V$ is regular. This yields a contradiction, so A has to be singular.

"$\Leftarrow$": Let A be singular. Then there exists a $u \neq 0$, $Au = 0$. If we write $u = V\tilde{p}+W\tilde{q}$ as in remark 2.1, then either $\tilde{p}$ or $\tilde{q}$ has to be nonzero. Since

$$0 = W^T Au = W^T AV\tilde{p} + W^T AW\tilde{q}$$

which yields by $W^T AW$ being invertible

$$\tilde{q} = -(W^T AW)^{-1}W^T AV\tilde{p},$$

$\tilde{p}$ can not be zero. From the definition of P_A one can see immediately that $V^T A P_A W \tilde{q} = 0$ for any $\tilde{q}$. Consequently,

$$0 = V^T A P_A u = V^T A P_A (V\tilde{p} + W\tilde{q}) = V^T A P_A V \tilde{p}.$$

Therefore $\bar{A}\tilde{p} = 0$ and $\bar{A}$ must be singular.

□

Remark 3.1. The bifurcation values, that is, the values of θ for which A and $\bar{A}$ become singular, are not to be confused with the eigenvalues of A and $\bar{A}$.

4. Numerical Results

The software package AUTO designed for the computation of bifurcation diagrams is used. In principle, it suffices to provide AUTO with the right hand side of the equation as input and AUTO will compute the diagram. However, since not only selected solutions but entire *families* of solutions must be computed for the diagram, the number of degrees of freedom of the system has to remain moderate due to memory limitation. For example, it is often not possible to deal with systems with several hundreds of degrees of freedom (cf [7]).

Assume now we want to obtain the bifurcation diagram of a certain finite difference semidiscretization (2.3) for some fixed number N of grid nodes. If N is prohibitively large, we have two choices. Firstly, we could just replace the grid by some coarser grid, that is, reduce N to some $n < N$. However, any essential information which cannot be resolved by the coarser grid would get lost. Secondly, we could reduce the number of degrees of freedom by replacing (2.3) by some AIF (2.10) and hope that the diagram of (2.10) will still capture the essential dynamics of (2.3). According to Lemma 3.1, at least the *primary* bifurcation values of (2.10) are exactly those of (2.3), so we can expect the diagrams of (2.3) and (2.10) to

coincide at least in a small horizontal strip around the horizontal line $\{\|u\| = 0\}$ of the bifurcation diagram.

For the numerical computations of the bifurcation diagrams in this section we have dropped the factor $(V^T V)^{-1}$ in the AIF (2.10). This is reasonable, since only steady states are computed in the diagrams.

4.1. **A simple reaction-diffusion equation.** We will compute the bifurcation diagram of the equilibria of the equation

$$u_t - u_{xx} - \theta(u + u^3) = 0 \tag{4.1}$$

on the spatial interval $[0, \pi]$ with zero boundary conditions $u(t, 0) = u(t, \pi) = 0$. By setting $\mu = \theta^{-1}$, $t = \mu s$ and $v(s, x) = u(t, x)$, equation (4.1) can be transformed to the classical Chaffee–Infante problem

$$v_s - \mu v_{xx} - v - v^3 = 0 \tag{4.2}$$

which has been studied rather extensively, see for example [14].

The primary bifurcation values θ of (4.1) are given by the eigenvalues of $-\partial^2/\partial x^2$, that is, $\theta_k = k^2, \quad k = 1, 2, \ldots$. For $\theta_k < \theta < \theta_{k+1}$ there are exactly k pairs of nontrivial equilibria $\varphi_0^{\pm}, \ldots, \varphi_{k-1}^{\pm}$, $\|\varphi_j^+\| = \|\varphi_j^-\|$. At $\theta = \theta_k$ a new branch of pairs of equilibria bifurcates from the trivial branch $u = 0$. There is no secondary bifurcation or bifurcation of any other kind in this system.

We semidiscretize (4.1) by the standard finite difference approximation with $h = \frac{\pi}{(N+1)}$

$$\frac{d}{dt}u_i + h^{-2}(-u_{i-1} + 2u_i - u_{i+1}) - \theta(u_i + u_i^3) = 0, \tag{4.3}$$

where $(u_1, \ldots, u_N)^T$ are the unknowns and u_i approximates $u(x, t)$ at $x = ih$ for $1 \le i \le N$. The boundary conditions are reflected by setting $u_0 = u_{N+1} = 0$ in the scheme. Writing the finite difference scheme in the matrix form, we have

$A = -\Delta_h - \theta I$, where

$$-\Delta_h = \frac{1}{h^2}\begin{pmatrix} 2 & -1 & & & \\ -1 & 2 & -1 & & \\ & \ddots & \ddots & \ddots & \\ & & -1 & 2 & -1 \\ & & & -1 & 2 \end{pmatrix}_{N\times N}.$$

Let $N = 2n+1$, we define p_i, q_i by (1.1) which can be written in the matrix form $p = V^T u$, $q = W^T u$ where

$$V^T = \frac{1}{4}\begin{pmatrix} 1 & 2 & 1 & & & \\ & 1 & 2 & 1 & & \\ & & \ddots & \ddots & \ddots & \\ & & & 1 & 2 & 1 \end{pmatrix}_{n\times N}, \quad W^T = \frac{1}{4}\begin{pmatrix} 2 & -1 & & & \\ -1 & 2 & -1 & & \\ & \ddots & \ddots & \ddots & \\ & & -1 & 2 & -1 \\ & & & -1 & 2 \end{pmatrix}_{(n+1)\times N}.$$

Calculating explicitly the quantities in (2.8), one finds

$$\begin{aligned}
16(Tu)_i &= u_{i-2} + 6u_i + u_{i+2}, \quad i = 1,\dots,N,\\
-16h^2(T\Delta_h u)_i &= -u_{i-3} + 2u_{i-2} - 7u_{i-1} + 12u_i - 7u_{i+1} + 2u_{i+2} - u_{i+3}, \quad i = 1,\dots,N,\\
-8h^2(V^T\Delta_h Vp)_i &= -p_{i-1} + 2p_i - p_{i+1}, \quad i = 1,\dots,n,\\
-16h^2(V^T\Delta_h Wq)_i &= q_{i-1} - q_i - q_{i+1} + q_{i+2}, \quad i = 1,\dots,n,\\
-16h^2(W^T\Delta_h Vp)_i &= p_{i-2} - p_{i-1} - p_i + p_{i+1}, \quad i = 1,\dots,n+1,\\
-8h^2(W^T\Delta_h Wq)_i &= 3q_{i-1} + 10q_i + 3q_{i+1}, \quad i = 1,\dots,n+1,\\
16(V^TVp)_i &= p_{i-1} + 6p_i + p_{i+1}, \quad i = 1,\dots,n,\\
16(W^TWq)_i &= q_{i-1} + 6q_i + q_{i+1}, \quad i = 1,\dots,n+1,
\end{aligned} \tag{4.4}$$

where the convention

$$\begin{aligned}
&p_0 = p_{n+1} = 0, \quad p_{-1} = -p_1, \quad p_{n+2} = -p_n, \quad q_0 = -q_1, \quad q_{n+2} = -q_{n+1},\\
&u_0 = u_{N+1} = 0, \quad u_{-1} = -u_1, \quad u_{-2} = -u_2, \quad u_{N+2} = -u_N, \quad u_{N+3} = -u_{N-1}
\end{aligned} \tag{4.5}$$

is used.

From the above calculation, one obtains that $\Delta_h T$, T and Δ_h are symmetric which leads to $AT = TA$ for the $A = -\Delta_h - \theta I$. Therefore, the IUs introduced in (2.8) will be used to calculate the bifurcation diagram.

The linear part of (2.10) (without the factor $(V^TV)^{-1}$) can be explicitly written out as:

$$\begin{aligned}
&\frac{d}{dt}p_i - \left(\frac{1}{8h^2} + \frac{\theta}{16}\right)(p_{i-1} + p_{i+1}) + \left(\frac{1}{4h^2} - \frac{3\theta}{8}\right)p_i \\
&\quad + \frac{1}{16h^2}(q_{i-1} - q_i - q_{i+1} + q_{i+2}) + f(p,q)_i = 0, \\
&\left(\frac{3}{8h^2} - \frac{\theta}{16}\right)(q_{i-1} + q_{i+1}) + \left(\frac{5}{4h^2} - \frac{3\theta}{8}\right)q_i \\
&\quad + \frac{1}{16h^2}(p_{i-1} - p_i - p_{i+1} + p_{i+2}) + g(p,0)_i = 0.
\end{aligned} \tag{4.6}$$

System (4.6) is an ODE system with n equations since the variables q is a function of p which is determined by the second equation. For any p, $g(p,0)_i$ can be evaluated using (2.9) and q can then be obtained by solving the second equation of (4.6).

Remark 4.1. Following the remark 2.2, we can prove that in the cases that $0 < h < \theta^{-1/2}$, the condition number of W^TAW is smaller than 6. In fact, one can write W^TAW explicitly

$$\begin{aligned}
(W^TAWq)_i &= bq_{i-1} + aq_i + bq_{i+1}, \quad 2 < i < n, \\
(W^TAWq)_1 &= (a-b)q_1 + bq_2, \\
(W^TAWq)_{n+1} &= bq_n + (a-b)q_{n+1}
\end{aligned}$$

where

$$a = \frac{5}{4h^2} - \frac{3\theta}{8}, \quad b = \frac{3}{8h^2} - \frac{\theta}{16}.$$

It is easy to check that a, b, $a-2b$ are positive. Since W^TAW is symmetric, by Gershgorin's Theorem all of its eigenvalues lie in the interval $[R_1, R_2]$ where

$$R_1 = a - 2b, \quad R_2 = \max\{a, a+2b\} = a + 2b.$$

Denoting $\delta = \theta h^2$, one can check that $0 \le \delta < 1$ which leads to

$$\kappa(W^TAW) \le \frac{a+2b}{a-2b} = 2\frac{\delta - 4}{\delta - 2} < 6.$$

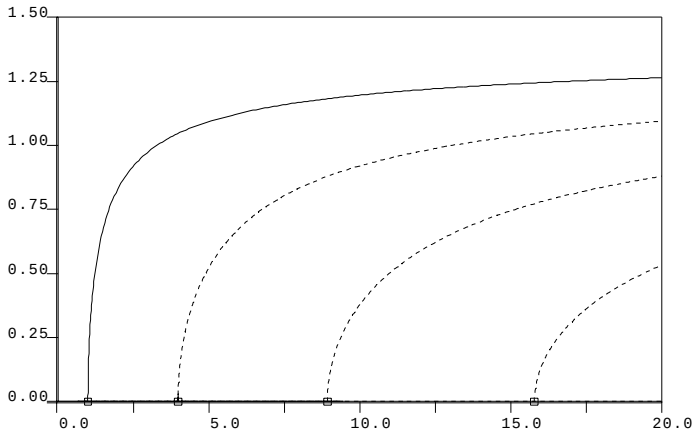

FIGURE 1. Bifurcation diagram of (4.3) with $N = 31$. The solid branch contains stable solutions, the dashed branches contain unstable solutions.

We made AUTO compute the bifurcation diagrams for (4.3) and (4.6) in the parameter range $0 \leq \theta \leq 20$ for various grids. Starting with the coarsest grid of only one inner grid point, we refined the grid until the computed primary bifurcation values were indistinguishable from the exact values $\theta_k = k^2$ in the diagram. It turned out that 4 refinement steps ($N = 31$ grid points) were necessary to obtain the desired accuracy. (see Fig. 1). We took the $N = 31$ diagram as the "reference diagram". Note that for three refinement steps ($N = 15$) the eigenvalues of $h^{-2}[-1, 2, -1]$ in $[0, 20]$ still differ substantially from the eigenvalues of the Laplacian which is shown in Fig. 2. Thus, reducing N from 31 to 15 produces larger errors in the higher primary bifurcation values. However, we see from Fig. 3 that a better result is obtained with only $n = 15$ degrees of freedom in the AIF. The $n = 15$ diagram is almost indistinguishable from the reference diagram, even for higher values of θ.

4.2. **The Kuramoto-Sivashinsky equation.** As a second example, we consider the Kuramoto-Sivashinsky equation

$$u_t + 4u_{xxxx} + \theta\,(u_{xx} + uu_x) = 0 \tag{4.7}$$

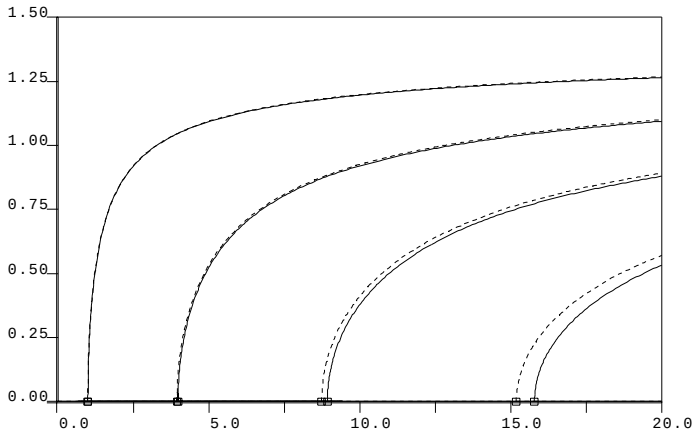

FIGURE 2. Bifurcation diagrams of (4.3) with $N = 15$ (dashed lines) and $N = 31$ (solid lines)

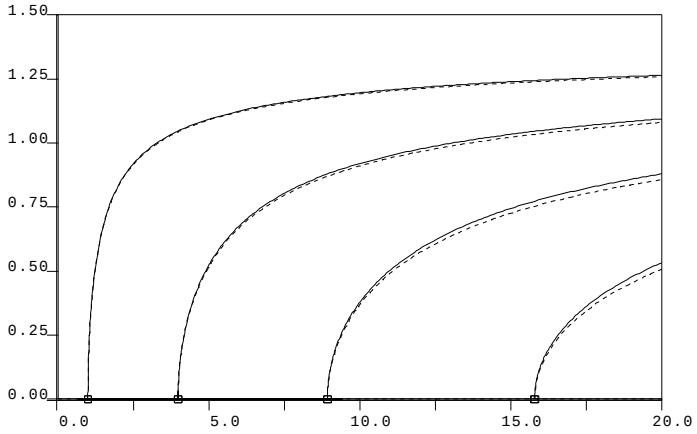

FIGURE 3. Bifurcation diagrams of (4.6) with $n = 15$ (dashed lines) and of (4.3) with $N = 31$ (solid lines)

on $H^{2,per}_{odd}(0, 2\pi)$. Equation (4.7) has been studied extensively and its bifurcation diagram in the parameter range $[0, 70]$ is certainly among the most often reproduced figures in dynamical systems literature of the past ten years ([15],[16], [19],[20],[26] and many more). Because only odd functions are considered, we may restrict the equation to the subspace of functions defined on $0 \leq x \leq \pi$ with $u(0) = u(\pi) = u''(0) = u''(\pi) = 0$.

The primary bifurcation values of (4.7) are those θ for which $4\Delta^2+\theta\Delta = \Delta(4\Delta+\theta)$ becomes singular. As Δ is nonsingular on this space, the primary bifurcation values are the eigenvalues of -4Δ which are given by $\theta_k = 4k^2, \quad k = 1, 2, \ldots$.

Replacing (4.7) by the semidiscretization, which has been proved to keep the dissipation property of the original K-S equation (4.7) (see [8]), one obtains

$$u_t + 4\Delta_h^2 u + \theta\,(\Delta_h u + F(u)) = 0 \tag{4.8}$$

where

$$(\Delta_h^2 u)_i = h^{-4}(u_{i-2} - 4u_{i-1} + 6u_i - 4u_{i+1} + u_{i+2}),$$

$$(\Delta_h u)_i = h^{-2}(u_{i-1} - 2u_i + u_{i+1}),$$

$$uu_x \simeq F(u) = \frac{u_{i+1} + u_i + u_{i-1}}{3} \cdot \frac{u_{i+1} - u_{i-1}}{2h},$$

$h = \pi/(N+1)$ and $(u_1, \ldots, u_N)^T$ are the unknowns which approximate $u(t,x)$ at $x = i * h$ for $i = 1, 2, \cdots, N$. According to the boundary conditions, we set $u_0 = u_{N+1} = 0$ and $u_{-1} = -u_1$, $u_{N+2} = -u_N$. As we proved in the preceding example, $\Delta_h T$, T and Δ_h are symmetric which leads to $AT = TA$ for $A = 4\Delta_h^2 + \theta\Delta_h$, so (2.10) with the IUs defined in (1.1) can be used to calculate the bifurcation diagram in this example as well.

The terms in (2.10) for the equation (4.8) can again be written explicitly (terms involving Δ_h has already been calculated in (4.4)).

$$16h^4(V^T\Delta_h^2 Vp)_i = p_{i-2} - 4p_{i-1} + 6p_i - 4p_{i+1} + p_{i+2}, \quad i = 1, \ldots, n$$

$$4h^4(V^T\Delta_h^2 Wq)_i = q_{i-1} - q_i - q_{i+1} + q_{i+2}, \quad i = 1, \ldots, n$$

$$4h^4(W^T\Delta_h^2 Vp)_i = p_{i-2} - p_{i-1} - p_i + p_{i+1}, \quad i = 1, \ldots, n+1$$

$$16h^4(W^T\Delta_h^2 Wq)_i = q_{i-2} + 28q_{i-1} + 70q_i + 28q_{i+1} + q_{i+2}, \quad i = 1, \ldots, n+1$$

where the same convention as in (4.5) and $q_{-1} = -q_2$, $q_{n+3} = -q_n$ are used.

The AIF of (4.8) (namely (2.10) for the K-S equation) is thus given by

$$\begin{aligned}
&\frac{d}{dt}p_i + \frac{1}{4h^4}(p_{i-2} - 4p_{i-1} + 6p_i - 4p_{i+1} + p_{i+2}) + \frac{\theta}{8h^2}(p_{i-1} - 2p_i + p_{i+1}) \\
&\quad + \left(\frac{1}{h^4} - \frac{\theta}{16h^2}\right)(q_{i-1} - q_i - q_{i+1} + q_{i+2}) + f(p,q)_i = 0, \\
&\quad \left(\frac{1}{h^4} - \frac{\theta}{16h^2}\right)(p_{i-2} - p_{i-1} - p_i + p_{i+1}) - \frac{\theta}{8h^2}(3q_{i-1} + 10q_i + 3q_{i+1}) \\
&\quad + \frac{1}{4h^4}(q_{i-2} + 28q_{i-1} + 70q_i + 28q_{i+1} + q_{i+2}) + g(p,0)_i = 0.
\end{aligned} \tag{4.9}$$

Remark 4.2. Similarly to the case of the first example, the linear equation for q has a condition number κ which is smaller than 12 independently of h if $h < \theta^{-1/2}$. In fact,

$$\begin{aligned}
(W^T AWq)_i &= cq_{i-2} + bq_{i-1} + aq_i + bq_{i+1} + cq_{i+2}, \quad 3 \le i \le n-1, \\
(W^T AWq)_1 &= (a-b)q_1 + (b-c)q_2 + cq_3, \\
(W^T AWq)_2 &= (b-c)q_1 + aq_2 + bq_3 + cq_4, \\
(W^T AWq)_n &= cq_{n-2} + bq_{n-1} + aq_n + (b-c)q_{n+1}, \\
(W^T AWq)_{n+1} &= cq_{n-1} + (b-c)q_n + (a-b)q_{n+1},
\end{aligned}$$

where

$$a = \frac{35}{2h^4} - \frac{5\theta}{4h^2}, \quad b = \frac{7}{h^4} - \frac{3\theta}{8h^2}, \quad c = \frac{1}{4h^4}.$$

Again for $h < \theta^{-1/2}$ it is easy to check that all a, b, c, $b-c$, $a-b$, $a-2b-2c$ are positive and that by Gershgorin's Theorem all of the eigenvalues of $W^T AW$ lie in the interval $[R_1, R_2]$ where

$$\begin{aligned}
R_1 &= \min\{a-2b-2c, a-2b\} = a-2b-2c, \\
R_2 &= \max\{a+2b+2c, a+2b, a\} = a+2b+2c,
\end{aligned}$$

so

$$\kappa \le \frac{a+2b+2c}{a-2b-2c} = 4\frac{\delta-16}{\delta-6} < 12$$

where $\delta = \theta h^2 < 1$.

Again, we made AUTO compute the bifurcation diagrams for the original scheme (4.8) and its AIF (4.9) and compared the diagrams. Following the same procedure, the bifurcation diagram of (4.8) with $N = 17$, which is shown in Fig. 4, is chosen to be the reference diagram. Fig. 4 is also compared with existing results. For instance, it is almost identical to Fig. 3.1 in [26] which was computed by a 12 mode classical spectral method. Reducing the number of grid points to $N = 8$ leads to major differences in the right part of the diagram (see Fig. 5). Therefore, $N = 8$ nodes is not sufficient to correctly reproduce the dynamics. Again, we see that a substantial improvement of the bifurcation diagram can be produced by taking $n = 8$ degrees of freedom in the AIF (see Fig. 6).

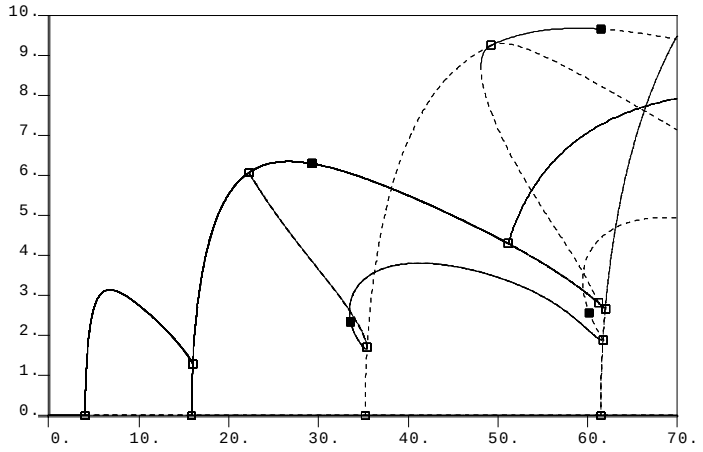

FIGURE 4. Bifurcation diagram of (4.8) with $N = 17$

Acknowledgements: Part of this work was done when R. Bronstering enjoyed the hospitalty of Pennsylvania State University. R. Bronstering was supported in part by the Deutsche Forschungsgemeinschaft (Grant BR 1714/2-1) and M. Chen was supported in part by NSF grants DMS-9410188 and DMS-9622858.

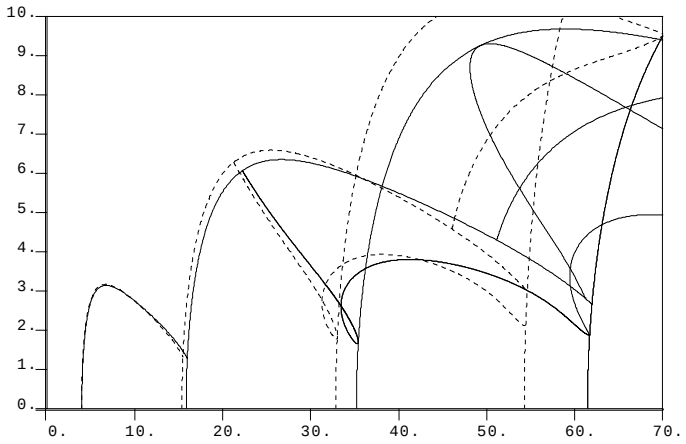

FIGURE 5. Bifurcation diagrams of (4.8) with $N = 8$ (dashed lines) and $N = 17$ (solid lines)

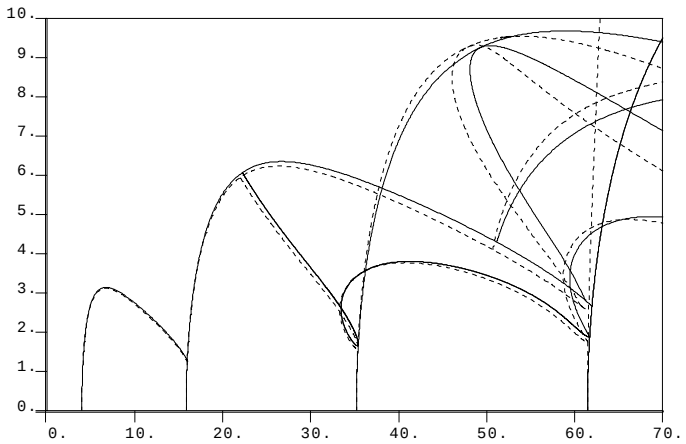

FIGURE 6. Bifurcation diagrams of (4.9) with $n = 8$ (dashed lines) and of (4.8) with $N = 17$ (solid lines)

References

[1] N. Aubry, W. Lian, and E.S. Titi. Preserving symmetries in the proper orthogonal decomposition. *SIAM J. Sci. Comp.*, 14:483–505, 1993.

[2] R. Bronstering. Some computational aspects on approximate inertial manifolds and finite differences. *Discrete and Continuous Dynamical Systems*, 2:417–454, 1996.

[3] M. Chen, H. Choi, T. Dubois, J. Shen, and R. Temam. The incremental unknowns–multilevel scheme for the simulation of turbulent channel flows. *Proceedings of 1996 Summer Program, Center for Turbulence Research, NASA Ames/Stanford Univ.*, pages 291–308, 1996.

[4] M. Chen and R. Temam. Incremental unknowns for solving partial differential equations. *Numerische Mathematik*, 59:255–271, 1991.

[5] M. Chen and R. Temam. Nonlinear galerkin method in the finite difference case and wavelet-like incremental-unknowns. *Numerische Mathematik*, 64(3):271–294, 1993.

[6] M. Chen and R. Temam. Nonlinear galerkin method with multilevel incremental-unknowns. In R. P. Agarwal, editor, *Contributions in Numerical Mathematics*, pages 151–164. WSSIAA, 1993.

[7] E. J. Doedel, X.J. Wang, and T.F.Fairgrieve. Software for continuation and bifurcation problems in ordinary differential equations. *CRPC-95-2, Center for Research on Parallel Computing, California Institute of Technology*, 1995.

[8] C. Foias, Jolly, Kevrekidis, and E.S. Titi. Dissipativity of numerical schemes. *Nonlinearity*, pages 591–613, 1991.

[9] C. Foias, O. Manley, and R. Temam. Modeling of the interaction of small and large eddies in two dimensional turbulent flows. *Math. Model. and Num. Anal.*, 22(1), 1988.

[10] C. Foias and E.S. Titi. Determining nodes, finite difference schemes and inertial manifolds. *Nonlinearity*, 4:135–153, 1991.

[11] G. Golub and C. van Loan. *Matrix Computations*. The John Hopkins University Press, second edition, 1989.

[12] J. Hale. *Asymptotic Behavior of Dissipative Systems*. AMS, 1988.

[13] J.M. Hyman, B. Nicolaenko, and S. Zaleski. Order and complexity in the kuramoto–sivashinsky model of weakly turbulent interfaces. *Physica D*, 23:265–292, 1986.

[14] M. Jolly. Explicit construction of an inertial manifold for a reaction diffusion equation. *J. Diff. Eq.*, 78:220–261, 1989.

[15] M.S. Jolly, I.G. Kevrekidis, and E.S. Titi. Approximate inertial manifolds for the kuramoto–sivashinsky equation: Analysis and computations. *Physica D*, 44:38–60, 1990.

[16] M.S. Jolly, I.G. Kevrekidis, and E.S. Titi. Preserving dissipation in approximate inertial forms for the kuramoto–sivashinsky equation. *J. Dyn. Diff. Eq.*, 3:179–197, 1991.

[17] D. A. Jones, L. G. Margolin, and E. S. Titi. On the effectiveness of the approximate inertial manifold-a computational study. *to appear in Theoretical and Computational Fluid Dynamics*, 1995.

[18] D.A. Jones, L.G. Margolin, and A.C. Poje. Enslaved finite difference schemes for nonlinear dissipative pdes. *Num. Meth. for PDEs*, page to appear.

[19] Kevrekidis, Nicolaenko, and Scovel. Back in the saddle again: A computer assisted study of the kuramoto–sivashinsky equation. *Siam J. Apl. Math.*, 50:760–790, 1990.

[20] E. Korontinis and M.R. Trummer. A finite difference scheme for computing inertial manifolds. *Z angew Math Phys*, 46:419–444, 1995.

[21] L.G. Margolin and D.A. Jones. An approximate inertial manifold for computing burger's equation. *Physica D*, 60:175–184, 1992.

[22] M. Marion. Approximate inertial manifolds for reaction–diffusion equations in high space dimension. *J Dyn. Diff. Eq.*, 1:245–267, 1989.

[23] M. Marion and R. Temam. Nonlinear galerkin methods. *SIAM J. Num. An.*, 26:1139–1157, 1989.

[24] B. Nicolaenko, B. Scheurer, and R. Temam. Some global dynamical properties of the kuramoto–sivashinsky equation: Nonlinear stability and attractors. *Physica D*, 16:155–183, 1985.

[25] R. Temam. *Infinite–Dimensional Dynamical Systems in Mechanics and Physics*. Springer Verlag, 1988.

[26] R. Wallace and D.M. Sloan. Numerical solution of a nonlinear dissipative system using a pseudospectral method and inertial manifolds. *Siam J. Sci. Comput.*, 16:1049–1070, 1994.